Solving continuum problems with bound state methods

Y. Suzuki (Niigata & RIKEN)

Progress in ab initio approach to bound states
Predictability

Problems involving continuum states are of increasing importance but are still difficult to solve generally

Application of bound state technique to continuum problems
Use of correlated ground state wave functions
→ These are vital to understand the dynamics of reactions

Problems including continuum states

Decay of resonance (stabilization, ACCC, etc.)

$A^* \longrightarrow B+b, \quad C+d+e$

- Strength (response) function due to perturbation W

  $A+W \longrightarrow A^*, \quad B+b, \quad C+d+e$

  Photodisintegration(photoabsorption) $C+\gamma \longrightarrow A+a$

  Inverse process (radiative capture)

  $A+a \longrightarrow C+\gamma$

- Two-body scattering and reactions

  $A+a \longrightarrow B+b$

Plan of a talk

Brief explanation of our square-integrable basis functions

Photoabsorption of ^{4}He
CSM compared to reaction calculations

Importance of distorted configurations in scattering
A+B, A*+B*, C*(A+B)

Radiative capture and transfer reactions of A=4 system
Microscopic R-matrix method
Revealing the role of tensor force through astrophysical S-factors

Difficulties in three-particle continuum problems

Explicitly correlated Gaussians (ECG)

Two strategies in ab initio studies (starting from realistic interactions)

Use of transformed Hamiltonian, easier to larger A (NCSM, UCOM, EIHH,…)

Use of original Hamiltonian, transparent to see interplay (GFMC, CHHM,…)

Variational method

$$\Psi^{\pi}_{JM_JTM_T} = \sum_{LS} C_{LS} \Psi^{\pi}_{(LS)JM_JTM_T}$$

Orbital functions with ECG +GVR

Spherical part

$$\tilde{\boldsymbol{x}} A \boldsymbol{x} = \sum_{i,j} A_{ij} \boldsymbol{x}_i \cdot \boldsymbol{x}_j$$

$$\exp\left[-\frac{1}{2}\sum_{i<j}\left(\frac{\boldsymbol{r}_i - \boldsymbol{r}_j}{b_{ij}}\right)^2\right] = \exp\left(-\frac{1}{2}\tilde{\boldsymbol{x}} A \boldsymbol{x}\right)$$

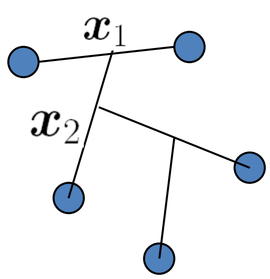

Angular part (Global vector)

$$\mathcal{Y}_{LM}(u_1\boldsymbol{x}_1 + u_2\boldsymbol{x}_2 + \ldots)$$

$L^{\pi} =$ 0^+, 1^-, 2^+, 3^- etc.

$$[\mathcal{Y}_{L_1}(u_1\boldsymbol{x}_1 + u_2\boldsymbol{x}_2 + \ldots)\mathcal{Y}_{L_2}(v_1\boldsymbol{x}_1 + v_2\boldsymbol{x}_2 + \ldots)]_{LM}$$

$L^{\pi} =$ 1^+, 2^-, 3^+ etc.

(L_1=L, L_2=1)

Variational parameters are determined by SVM

Characteristics of ECG

◯ Analytic evaluation of matrix elements
◎ Coordinate transf. & permutations keep ECG
◯ Versatility in describing different shapes
◯ Momentum rep. is again ECG
× Uneconomical to cope with SR repulsion

'cluster-like state'

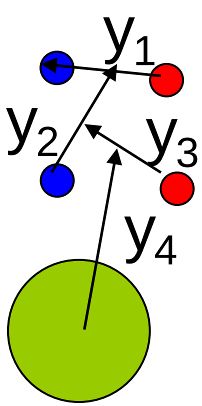

'shell-model like state'

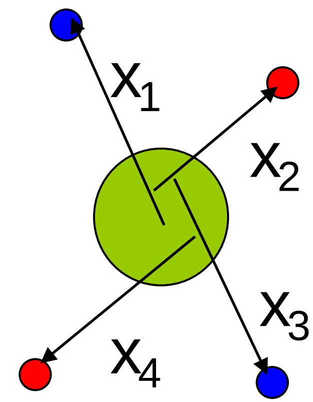

$$\exp\Big(-\frac{1}{2}\tilde{\boldsymbol{y}}B\boldsymbol{y}\Big)\mathcal{Y}_{LM}(v_1\boldsymbol{y}_1+v_2\boldsymbol{y}_2+\ldots) \;=\; \exp\Big(-\frac{1}{2}\tilde{\boldsymbol{x}}A\boldsymbol{x}\Big)\mathcal{Y}_{LM}(u_1\boldsymbol{x}_1+u_2\boldsymbol{x}_2+\ldots)$$

$$\boldsymbol{y}=T\boldsymbol{x} \quad\Longrightarrow\quad \tilde{\boldsymbol{y}}B\boldsymbol{y}=\tilde{\boldsymbol{x}}\widetilde{T}BT\boldsymbol{x} \qquad A=\tilde{T}BT$$

$$\tilde{v}\boldsymbol{y}=\widetilde{\tilde{T}v}\boldsymbol{x} \qquad u=\tilde{T}v$$

reduce to a choice of A, u

(cf. No need of explicit inclusion of rearrangement channels)

PWE $e^{-a_1 \boldsymbol{x}_1^2 - a_2 \boldsymbol{x}_2^2 - a_3 \boldsymbol{x}_3^2 - \cdots} \; [[[\mathcal{Y}_{L_1}(\boldsymbol{x}_1) \times \mathcal{Y}_{L_2}(\boldsymbol{x}_2)]_{L_{12}} \times \mathcal{Y}_{L_3}(\boldsymbol{x}_3)]_{L_{123}} \cdots]_{LM}$

(Product form of 's.p.' orbits Rearrangement channels must be included)

	Potential	MN	G3RS		AV8′		
	Method	GVR	GVR	PWE	GVR	PWE	ref. [26]
^{3}H$(\frac{1}{2}^+)$	E	−8.38	−7.73	−7.72	−7.76	−7.76	−7.767
	$\langle T \rangle$	27.21	40.24	40.22	47.59	47.57	47.615
	$\langle V_c \rangle$	−35.59	−26.80	−26.79	−22.50	−22.49	−22.512
	$\langle V_t \rangle$	–	−21.13	−21.13	−30.85	−30.84	−30.867
	$\langle V_b \rangle$	–	−0.03	−0.03	−2.00	−2.00	−2.003
	$\sqrt{\langle r^2 \rangle}$	1.71	1.79	1.79	1.75	1.75	
$P(L,S)$ (%)	$P(0,\frac{1}{2})$	100	92.95	92.94	91.38	91.37	91.35
	$P(2,\frac{3}{2})$	–	7.01	7.02	8.55	8.57	8.58
	$P(1,\frac{1}{2})$	–	0.03	0.03	0.04	0.04	$\}$ 0.07
	$P(1,\frac{3}{2})$	–	0.02	0.02	0.02	0.02	
^{4}He(0^+)	E	−29.94	−25.29	−25.29	−25.09	−25.05	
	$\langle T \rangle$	58.08	86.93	86.90	101.62	101.41	
	$\langle V_c \rangle$	−88.86	−66.24	−66.19	−54.93	−54.76	
	$\langle V_{Coul} \rangle$	0.83	0.76	0.76	0.77	0.77	
	$\langle V_t \rangle$	–	−46.62	−46.65	−67.89	−67.82	
	$\langle V_b \rangle$	–	−0.13	−0.12	−4.66	−4.66	
	$\sqrt{\langle r^2 \rangle}$	1.41	1.51	1.51	1.49	1.49	
	$P(0,0)$	100	88.46	88.45	85.76	85.79	
	$P(2,2)$	–	11.30	11.30	13.88	13.85	
	$P(1,1)$	–	0.25	0.24	0.36	0.36	

Y.S., W.Horiuchi, M.Orabi, K. Arai, FBS42(2008)

ECG + SVM

Convergence of the ground and first excited 0^+ states in ^{4}He

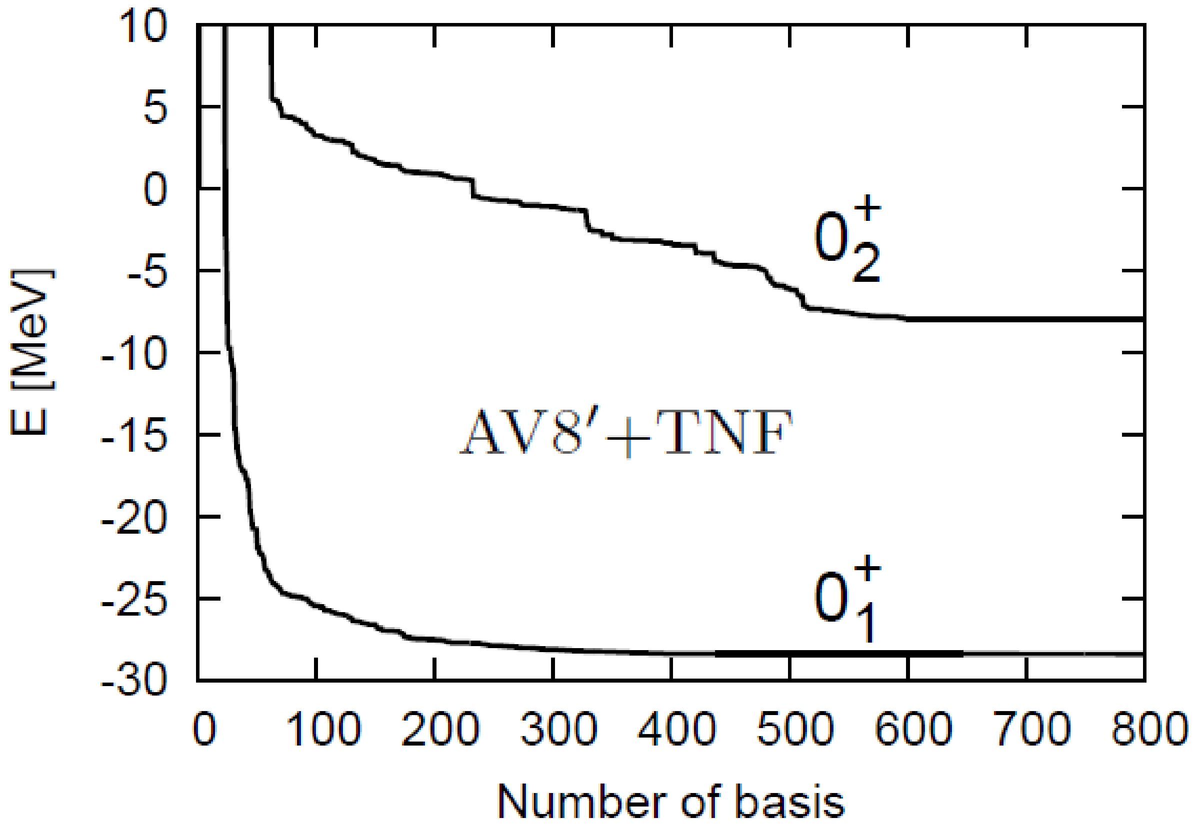

Photoabsorption cross section of ^{4}He

Interest: E1 strength in continuum (Γof 1^- ,T=1 states ～6, 12 MeV)

Excited states obtained with realistic interaction

Experiments in discrepancy

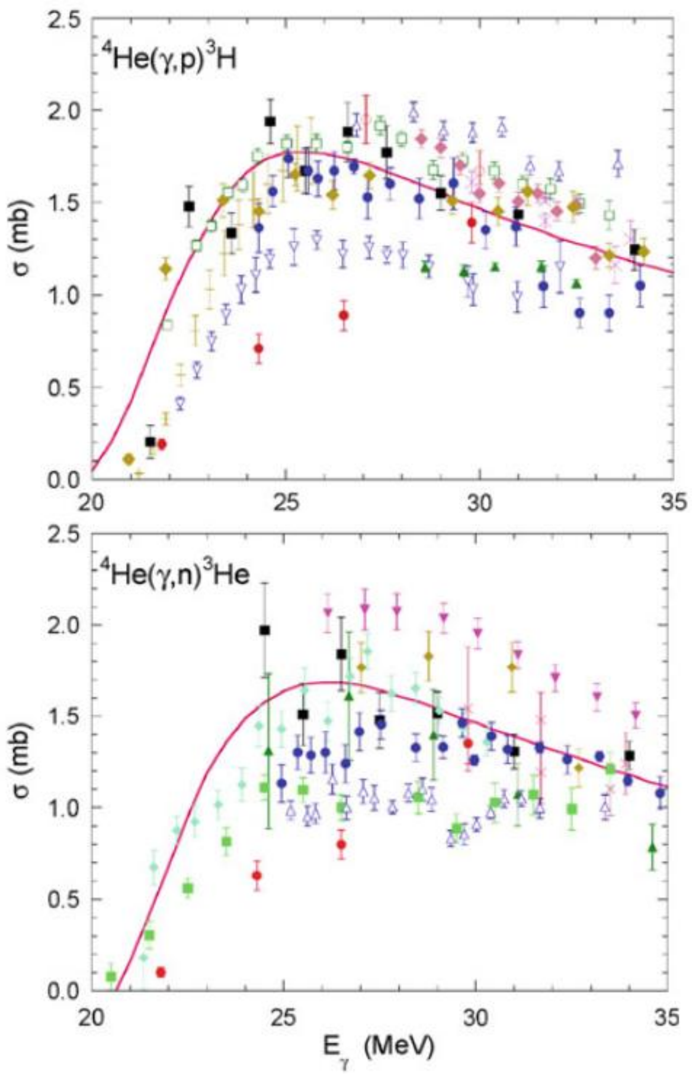

W.Horiuchi, Y.S. PRC78(2008)

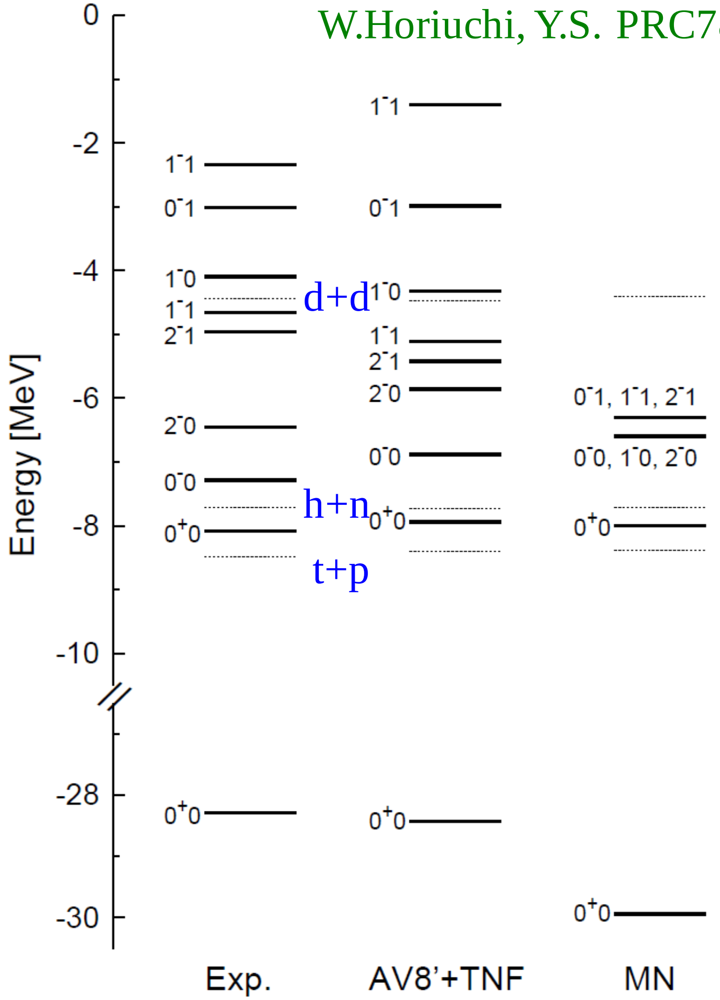

Contents responsible for level splitting

TABLE II: Energy contents, given in MeV, of the negative-parity states of ^{4}He. AV8′+TNF potential is used.

$J^\pi T$	$\langle H \rangle$	$\langle T \rangle$	$\langle V_c \rangle$	$\langle V_{\mathrm{Coul}} \rangle$	$\langle V_t \rangle$	$\langle V_b \rangle$	$\langle V_{\mathrm{TNF}} \rangle$
0^-0	−6.88	59.40	−24.85	0.51	−39.02	−1.61	−1.32
0^-1	−2.99	45.13	−21.29	0.45	−25.32	−1.07	−0.89
2^-0	−5.86	51.18	−21.57	0.45	−32.68	−2.31	−0.94
2^-1	−5.42	48.70	−22.66	0.45	−29.13	−1.94	−0.84
1_1^-1	−5.11	47.21	−21.97	0.44	−28.43	−1.61	−0.74
1^-0	−4.32	45.70	−20.47	0.41	−27.70	−1.60	−0.67
1_2^-1	−1.40	36.75	−18.87	0.43	−18.08	−0.92	−0.71

Photoabsorption and radiative capture

$\gamma + {}^4\text{He} \rightarrow {}^3\text{H}+\text{p}$

${}^3\text{He}+\text{n}$

${}^2\text{H}+\text{p}+\text{n}$

${}^3\text{H}+\text{p} \rightarrow {}^4\text{He}+\gamma$

Strength function and photoabsorption cross section

$$S(E) = \frac{1}{2J_i+1}\sum_{M_i\mu J_f M_f} |\langle \Psi_{J_f M_f}|\mathcal{M}_{\lambda\mu}|\Psi_{J_i M_i}\rangle|^2 \delta(E_f - E_i - E)$$

$$= -\frac{1}{\pi}\frac{1}{2J_i+1}\sum_{M_i\mu} \mathrm{Im}\langle \Psi_{J_i M_i}|\mathcal{M}^{\dagger}_{\lambda\mu}\frac{1}{E-H+i\varepsilon}\mathcal{M}_{\lambda\mu}|\Psi_{J_i M_i}\rangle$$

$$\sigma_\gamma(E) = \frac{4\pi^2}{\hbar c} E S(E)$$

Detailed balance $$\frac{v_1\sigma_{1\to 2}}{\rho_2} = \frac{v_2\sigma_{2\to 1}}{\rho_1}$$

From radiative capture cross section to photoabsorption cross section

$$\sigma_{\text{cap}}(E) = \frac{2J_f+1}{(2I_1+1)(2I_2+1)}\frac{8\pi}{\hbar}\left(\frac{E_\gamma}{\hbar c}\right)^{2\lambda+1}\frac{(\lambda+1)}{\lambda(2\lambda+1)!!^2} \times \sum_{J_i I_i \ell_i}\frac{1}{(2\ell_i+1)}\left|\langle \Psi^{J_f\pi_f}||\mathcal{M}^E_\lambda||\Psi^{J_i\pi_i}_{\ell_i I_i}(E)\rangle\right|^2, \quad \rightarrow \quad \sigma_\gamma(E)$$

Complex scaling method

Continuum state is made to damp asymptotically

$$U(\theta) \qquad \boldsymbol{x} \longrightarrow \mathrm{e}^{i\theta}\boldsymbol{x} \qquad\qquad \mathrm{e}^{i\boldsymbol{k}\cdot\boldsymbol{x}} \longrightarrow \mathrm{e}^{(-\sin\theta + i\cos\theta)\boldsymbol{k}\cdot\boldsymbol{x}}$$

Ideally applicable in atomic physics $\quad T \rightarrow T\mathrm{e}^{-2i\theta} \qquad \frac{1}{r} \longrightarrow \frac{1}{r}\mathrm{e}^{-i\theta}$

$$S(E) = -\frac{1}{\pi}\frac{1}{2J_i+1}\sum_{M_i\mu}\mathrm{Im}\langle\Psi_{J_iM_i}|\mathcal{M}^{\dagger}_{\lambda\mu}U^{-1}(\theta)R(\theta)U(\theta)\mathcal{M}_{\lambda\mu}|\Psi_{J_iM_i}\rangle$$

$$\begin{aligned} R(\theta) &= \frac{1}{E - H(\theta) + i\varepsilon} \\ &= \sum_{\lambda}\frac{1}{E - E^{\lambda}(\theta) + i\varepsilon}|\Psi^{\lambda}(\theta)\rangle\langle\tilde{\Psi}^{\lambda}(\theta)| \end{aligned}$$

$$H(\theta) = U(\theta)HU^{-1}(\theta)$$

$$\tilde{\Psi}^{\lambda}(\theta) = (\Psi^{\lambda}(\theta))^{*}$$

$$\boxed{H(\theta)\Psi^{\lambda}(\theta) = E^{\lambda}(\theta)\Psi^{\lambda}(\theta)} \qquad\qquad \int(\Psi^{\lambda}(\theta))^2 d\boldsymbol{x} = 1$$

Non-Hermitean, but can be diagonalized in L^2 basis
Stability of S(E) wrt θ is examined

Complex energy plane

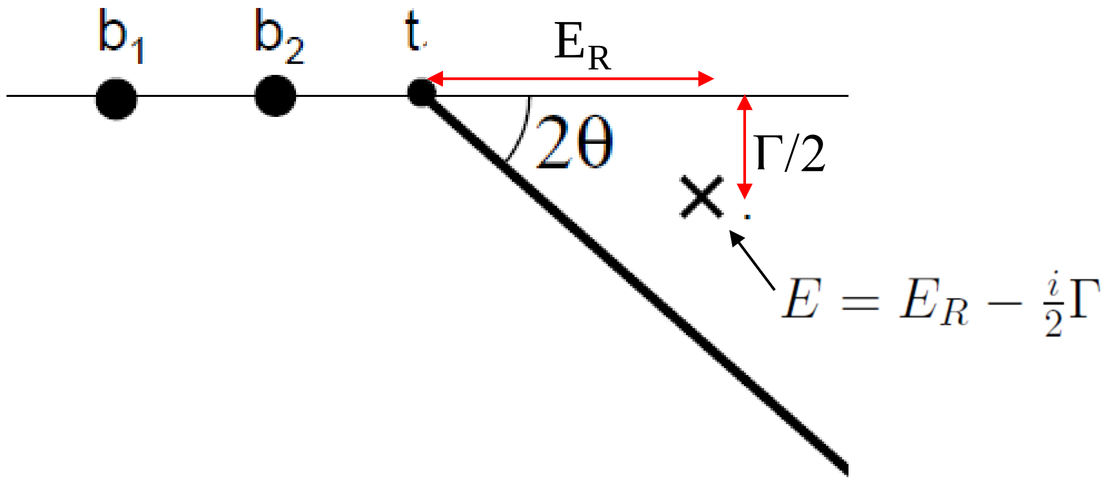

- To cover the resonance $\theta \sim \frac{1}{2}\arctan(\Gamma/2E_R)$
- $e^{-\rho r} \longrightarrow e^{-\rho r(\cos\theta + i \sin\theta)}$

  Potential range increases to $\rho\cos\theta$

Rotation by large angles may lead to instability

Calculation of photoabsorption cross section

CSM

Assume electric dipole transition

$$\mathcal{M}_{1\mu} = \sum_{i=1}^{4} \frac{e}{2}(1-\tau_{3i})(\boldsymbol{r}_i - \boldsymbol{x}_4)_\mu$$

basis states for 1^-, T=1

- 'Goldhaber–Teller' type (ED)

(E1 sum rule) $\mathcal{M}_1|\mathrm{Gnd}\rangle$

$$|\text{Gnd state of } {}^4\text{He}\rangle \sim |(L=0,S=0)J=0,T=0\rangle + |(L=2,S=2)J=0,T=0\rangle$$

$$|([(L=0,S=0)J'=0]\times\mathcal{M}_1)J=1,T=1\rangle$$

$$|([(L=2,S=2)J'=0]\times\mathcal{M}_1)J=1,T=1\rangle$$

- 3N + N cluster type
- 3N* + N cluster type

(Final state asymptotics)

$$|\tfrac{1}{2}(3N)\times(\mathcal{M}_1, S=\tfrac{1}{2})_j)J=1,T=1\rangle$$

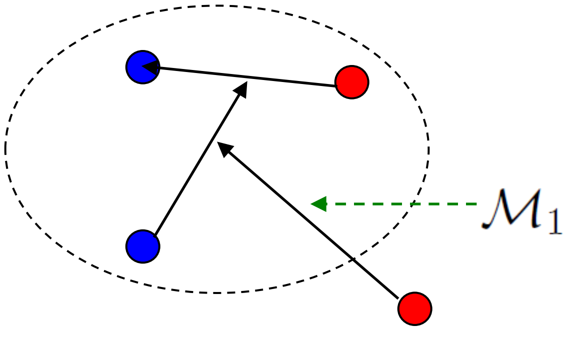

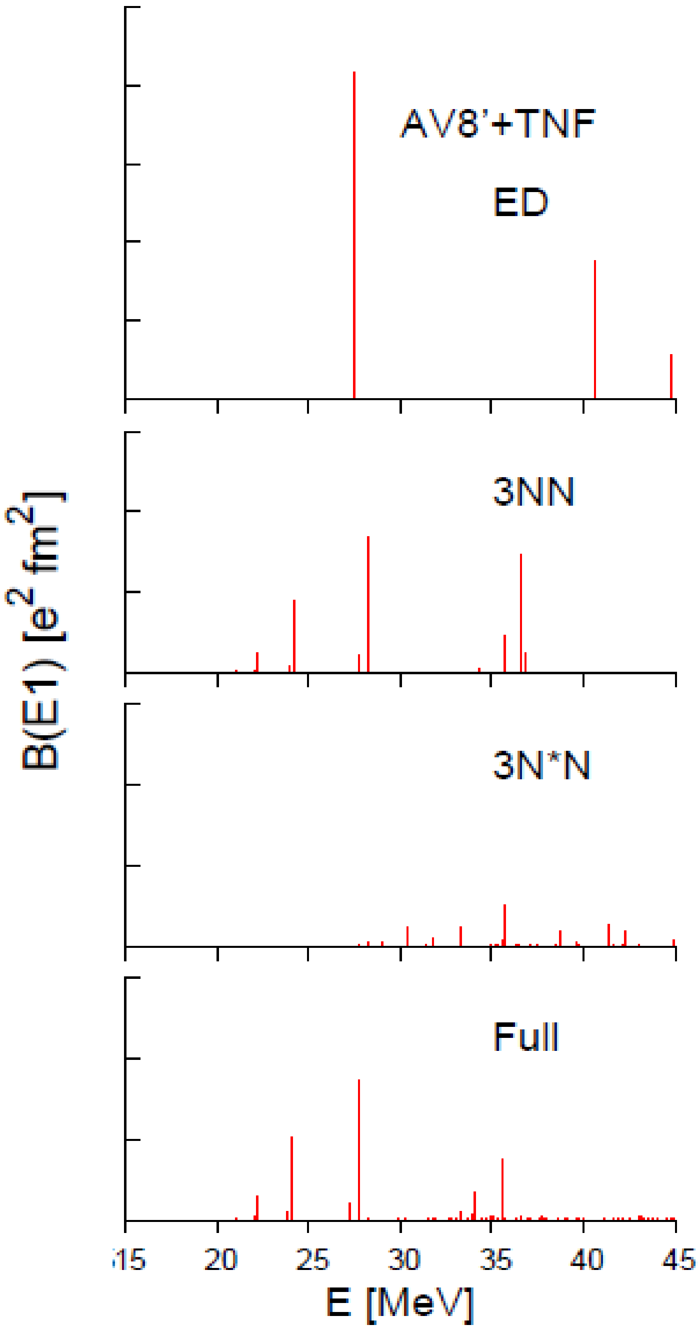

Microscopic calculation with realistic interaction

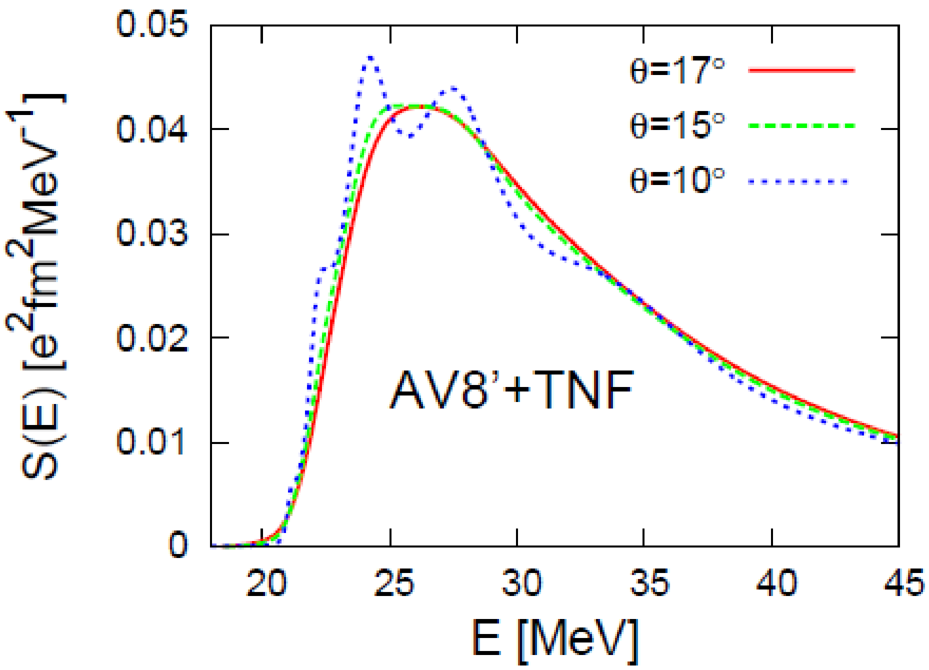

Energy average procedure not needed!

Comparison with radiative capture cross section

Microscopic R-matrix method (MRM) used to obtain scattering states
CSM and MRM agree very well, but in strong disagreement with experiments by Shima et al.

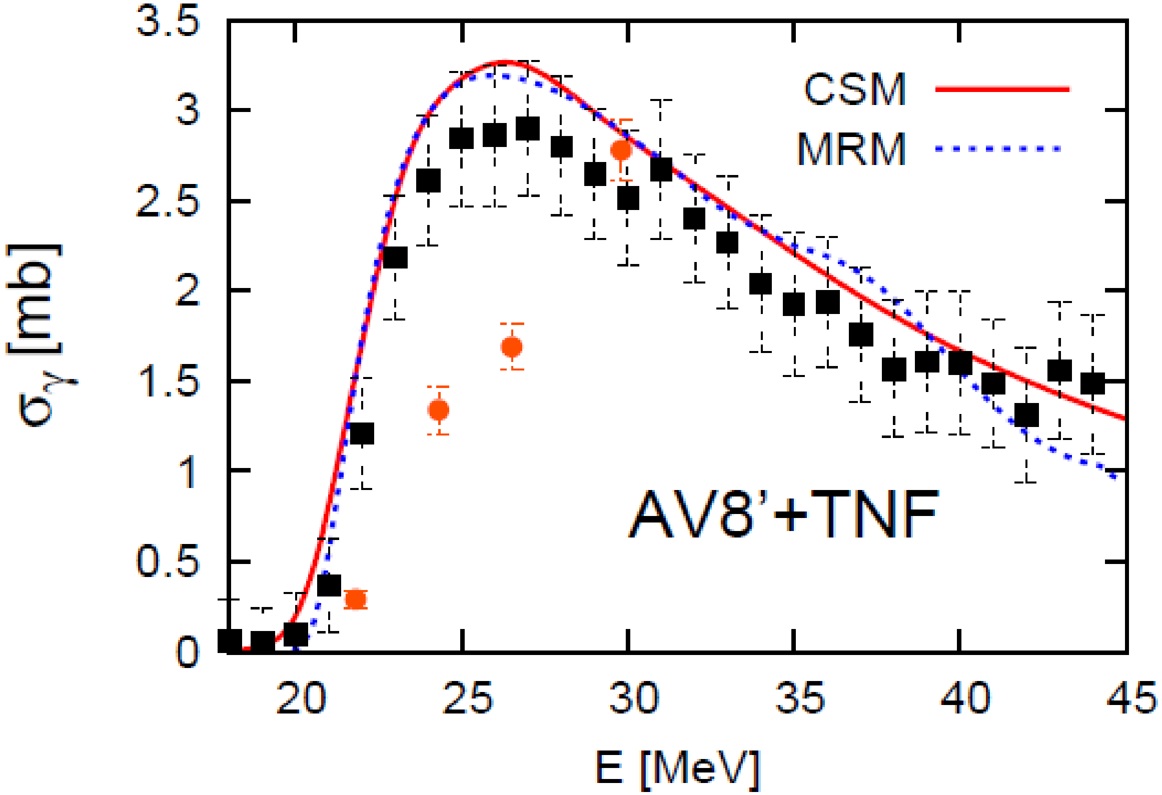

W.Horiuchi, Y.S., K.Arai, in preparation

Lorentz integral transform method

Lorentian weight

V.D.Efros, W.Leidemann, G.Orlandini, PLB338 (1994)

$$\mathcal{L}(z) = \int_{E_{\min}}^{\infty} \frac{S(E)}{(E-z)(E-z^*)} dE = \int_{E_{\min}}^{\infty} \frac{S(E)}{(E-E_R)^2 + E_I^2} dE$$

$$z = E_R + iE_I$$

$$\mathcal{L}(z) = \frac{1}{2J_i+1} \sum_{M_i\mu} \langle \Psi_{M_i\mu}(z) | \Psi_{M_i\mu}(z) \rangle$$

$$\Psi_{M_i\mu}(z) = \frac{1}{H - E_i - z} \mathcal{M}_{\lambda\mu} \Psi_{J_i M_i}$$

$$\boxed{(H - E_i - z)\Psi_{M_i\mu}(z) = \mathcal{M}_{\lambda\mu} \Psi_{J_i M_i}}$$

L(z) is finite, hence the norm of Ψ(z) is finite
Ψ(z) can be obtained in L^2 basis
L(z) has to be computed for many z values (E_R varied, E_I fixed)
to make the inversion possible

The inversion from L(z) to S(E) demands professional skill

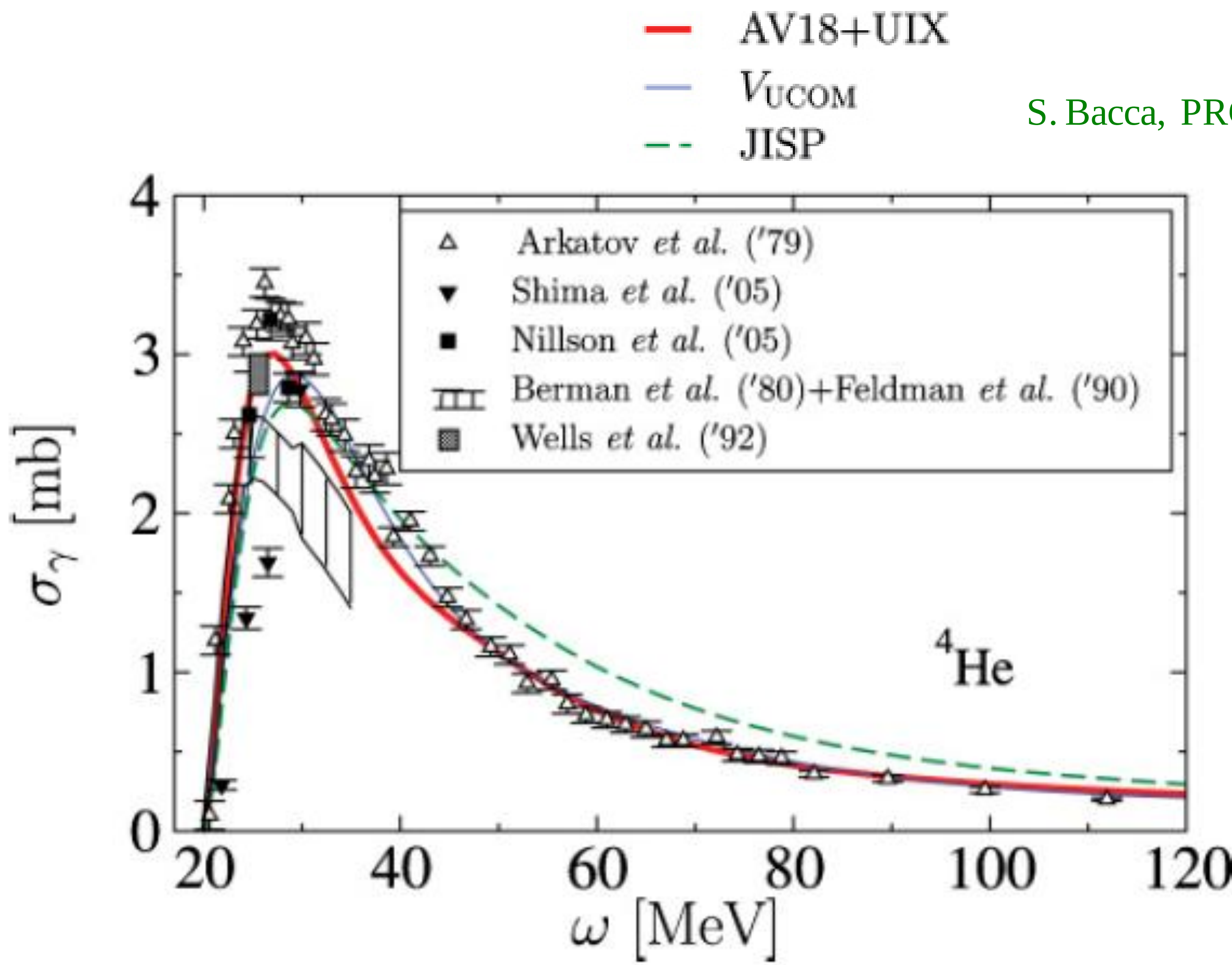

S. Bacca, PRC75 (2007)

Both CSM and LIT are successful.
Some sensitivity to the interactions
Advantage and disadvantage of CSM and LIT?

Laplace transform of strength function

J.Carlson, R.Schiavilla, PRL68 (1992)

$$\begin{aligned}\mathcal{L}(\tau) &= \int_{E_{\rm min}}^{\infty} \mathrm{e}^{-\tau E} S(E)\, dE \\ &= \frac{1}{2J_i+1} \sum_{M_i\mu} \langle \Psi_{J_iM_i} | \mathcal{M}^{\dagger}_{\lambda\mu} \mathrm{e}^{-\tau(H-E_i)} \mathcal{M}_{\lambda\mu} | \Psi_{J_iM_i} \rangle\end{aligned}$$

GFMC calculation

Scattering and reactions

$$\boxed{H\Psi^{\pi}_{JM} = E\Psi^{\pi}_{JM} \quad \text{with appropriate boundary condition}}$$

Simple case: single-channel

$$\Phi^{\pi}_{\alpha JM} = [[\Psi_{I_a} \times \Psi_{I_b}]_I \times Y_\ell(\hat{x}_\alpha)]_{JM}$$ Channel wave function

$$y_\alpha(r) = \langle \Phi^{\pi}_{\alpha JM} | \Psi^{\pi}_{JM} \rangle$$ **Spectroscopic amplitude** (SA)

(within a factor)

$$H = H_a + H_b + T_\alpha + V_\alpha \qquad \chi_\alpha(r) = r\, y_\alpha(r)$$

$$\boxed{\left[\frac{d^2}{dr^2} - \frac{\ell(\ell+1)}{r^2} - \frac{2\mu_\alpha}{\hbar^2} U_\alpha(r) + k_\alpha^2\right] \chi_\alpha(r) = \frac{2\mu_\alpha}{\hbar^2} r [z_\alpha(r) + w_\alpha(r)]}$$

$$z_\alpha(r) = \langle \Phi^{\pi}_{\alpha JM} \mid V_\alpha - U_\alpha \mid \Psi^{\pi}_{JM} \rangle$$

$$w_\alpha(r) = \langle \Phi^{\pi}_{\alpha JM} \mid H_a - E_{I_a} + H_b - E_{I_b} \mid \Psi^{\pi}_{JM} \rangle$$

$U_\alpha(r) = Z_a Z_b e^2 / r$ For $r > R$ $z, w \to 0$

$\Psi^{\pi}_{JM} \to \widetilde{\Psi}^{\pi}_{JM}$ Discretized solution at energy E, which is approximated well in internal region

Green's function method

$$\chi_\alpha(r) = \frac{2\mu_\alpha}{\hbar^2}\int_0^\infty G_\alpha(r,r')r'[z_\alpha(r') + w_\alpha(r')]dr'$$

$$\chi_\alpha(r) \sim I_\alpha(r) - SO_\alpha(r)$$

$$\tilde{\chi}_\alpha(r) = r\langle\Phi^\pi_{\alpha JM}|\widetilde{\Psi}^\pi_{JM}\rangle \sim \chi_\alpha(r)$$ for r < R

Y.S., W.Horiuchi,K.Arai, NPA823(2009)

α+n scattering

$$\tilde{\Psi}^\pi_{JM} = \sum_i C_i \mathcal{A}[[\Psi(\alpha)\Psi(n)]_{1/2}Y_\ell(\hat{\boldsymbol{r}})]_{JM}u_i(r)$$

$$u_i(r) = r^\ell \exp(-\beta_i r^2)$$

Single-channel approximation
No distortion included

Use of the wave function solved for α
Relative motion discretized

Minnesota force

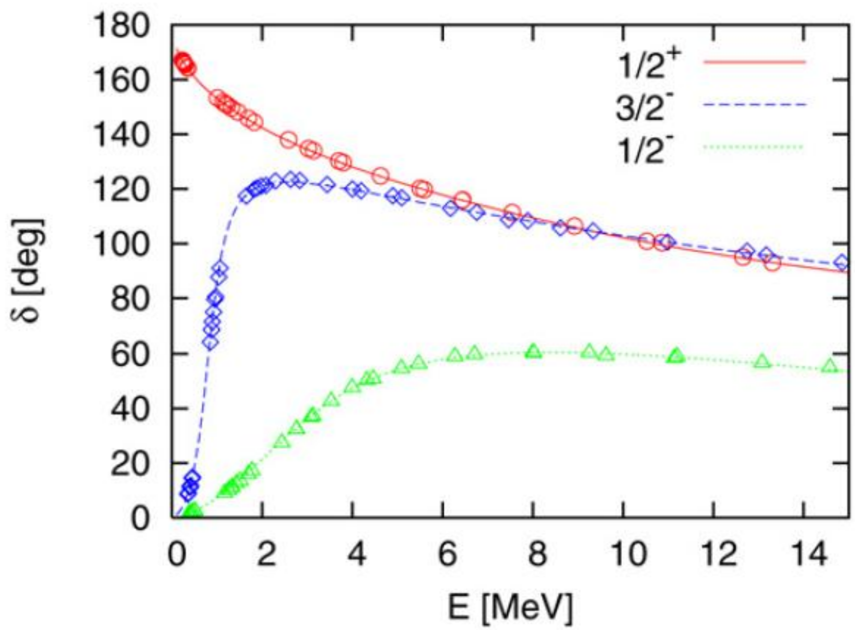

Green's function method agrees with MRM cal.

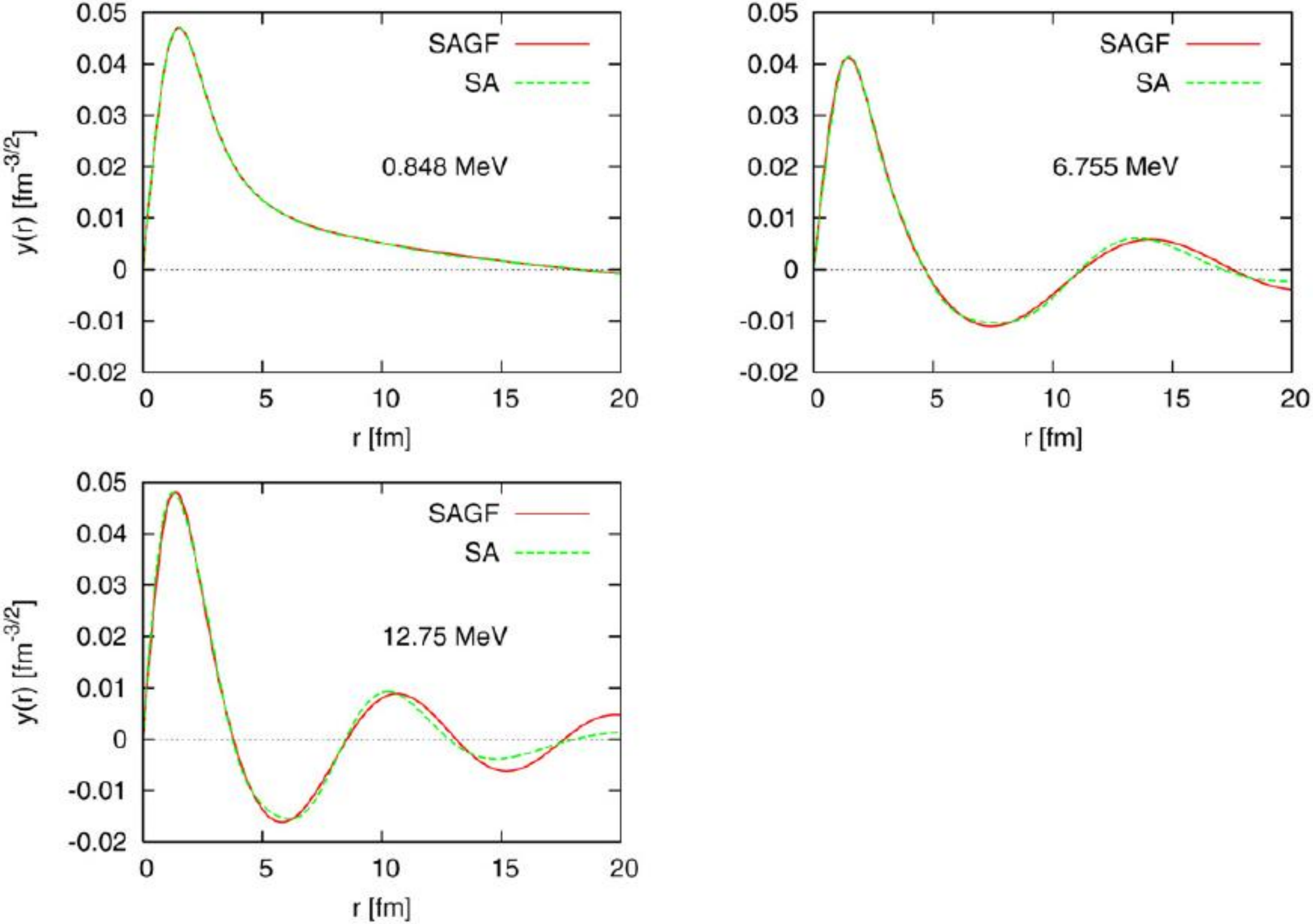
SAGF
SA
0.848 MeV
6.755 MeV
12.75 MeV
y(r) [fm^-3/2]
r [fm]
0.05
0.04
0.03
0.02
0.01
0
-0.01
-0.02
0
5
10
15
20

Comparison with empirical phase shifts

AV8' force

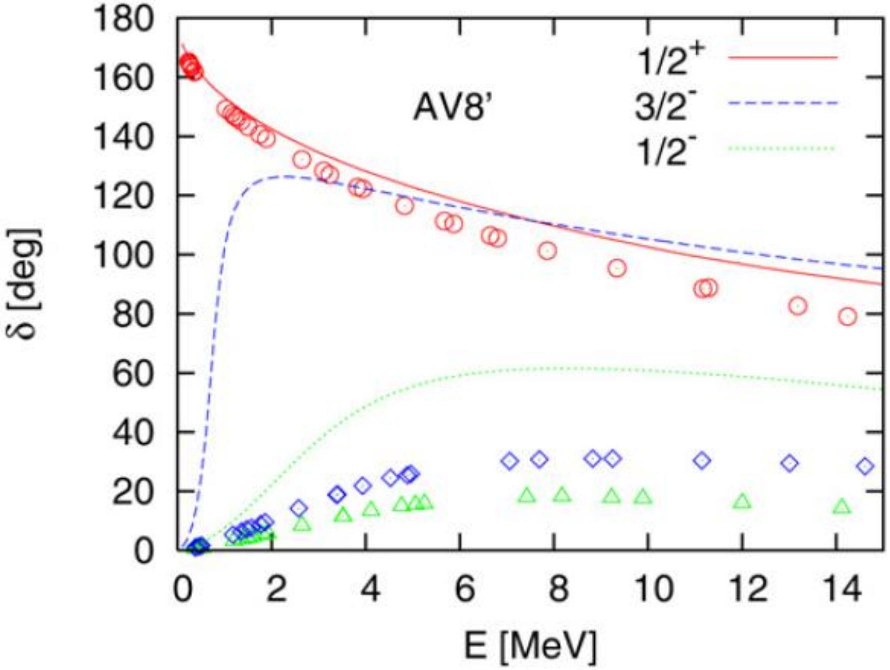

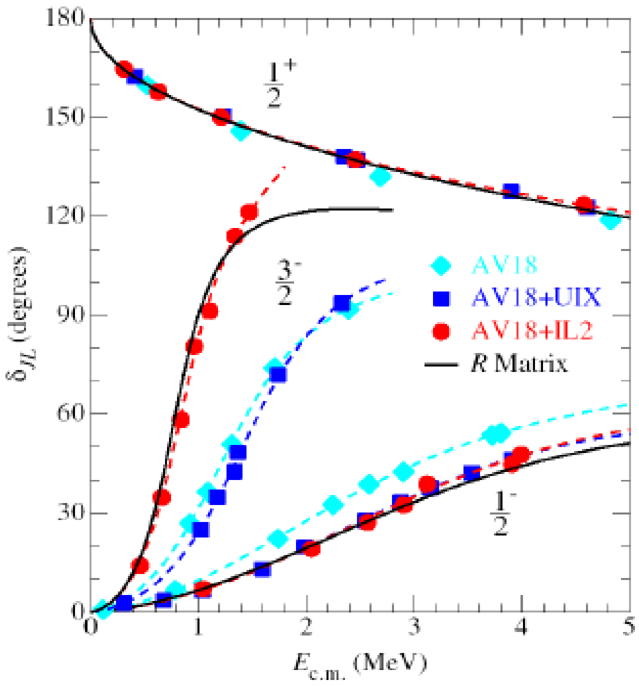

Quite different between effective and realistic interactions

Single-channel approximation breaks down esp. for P-wave

Distortion of nuclei (e.g., due to tensor force)

3NF K.M.Nollett et al., PRL99(2007)

^{3}He+p P-wave scattering

K.Arai, S.Aoyama, Y.S., PRC81(2010)

I=0, 1 $\quad \ell = 1 \qquad S_{\alpha\alpha} = \eta_\alpha \mathrm{e}^{2i\delta_\alpha}$

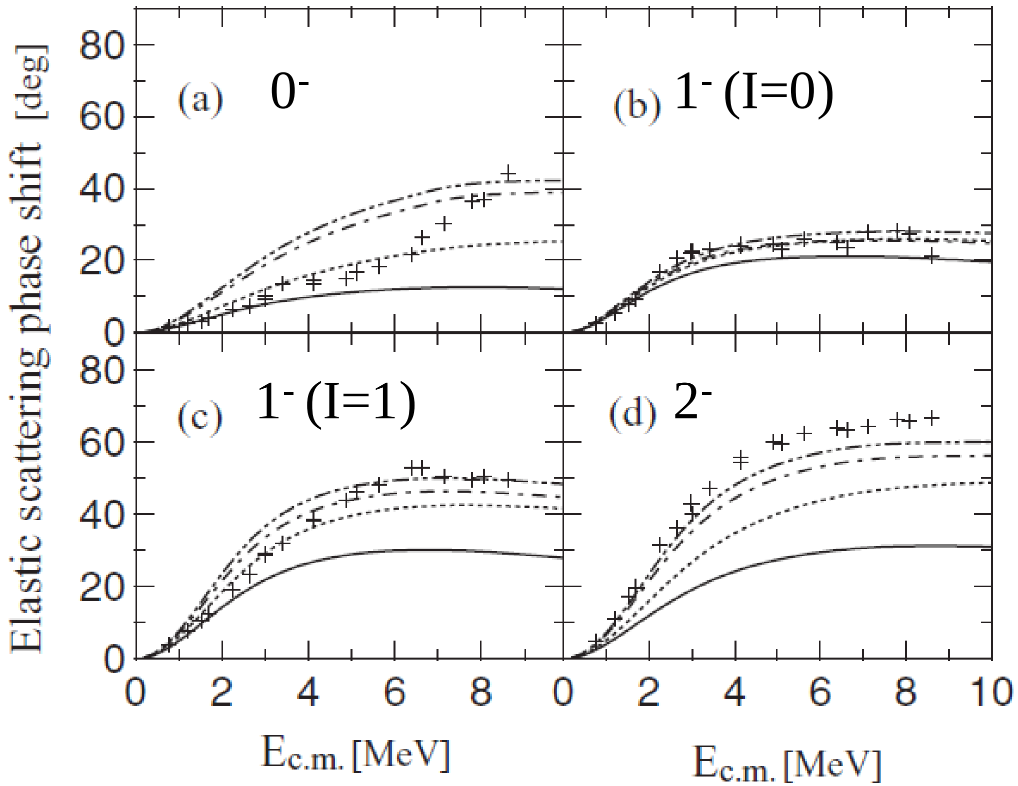

Improvement by including effects of distortion (pseudo configurations)

$^3\mathrm{He}(1/2^+) + p$ (solid line)

$^3\mathrm{He}(1/2^\pm, 3/2^\pm, 5/2^\pm) + p \quad d(0^+, 1^+) + 2p(0^+)$

Improving the solution in the interaction region is vital esp. for realistic interactions

1. To add many more channels (standard approach)
2. To solve A-body Schroedinger eq. more accurately in a confined region

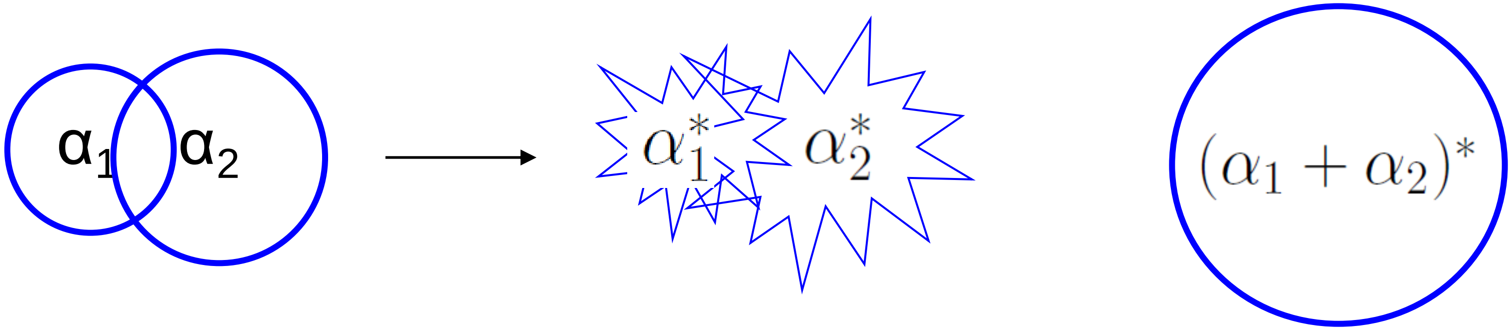

Microscopic R-matrix method

P.Descouvemont, D.Baye, Rep.Prog.Phys.73(2010)

$$(H + \mathcal{L} - E)\Psi^{\pi}_{\mathrm{int}JM} = \mathcal{L}\Psi^{\pi}_{\mathrm{ext}JM} \qquad r_a \le R$$

$$\Psi^{\pi}_{\mathrm{int\,JM}} = \Psi^{\pi}_{\mathrm{ext\,JM}} \quad \text{at } r_a = R$$

Bloch operator $\mathcal{L} = \sum_{\alpha} \frac{\hbar^2}{2\mu_\alpha R} |\Phi^{\pi}_{\alpha JM}\rangle \delta(r_\alpha - R)\left(\frac{\partial}{\partial r_\alpha} - \frac{b_\alpha}{r_\alpha}\right) r_\alpha \langle \Phi^{\pi}_{\alpha JM}|$

Kinetic energy is rendered Hermitean in the internal region
Derivatives of the internal and external wave functions are connected

$$\Psi^{\pi}_{\mathrm{int\,JM}} = \sum_i \Psi^{\pi}_{i\,JM}$$ Expansion in L^2 basis

$$\Psi^{\pi}_{\mathrm{ext\,JM}} = \sum_\alpha g_\alpha(r_\alpha)\Phi^{\pi}_{\alpha\,JM}$$ Expansion in channel components

Application of MRM to d-induced reactions on ^{2}H at astrophysical energy

Radiative capture $^{2}H(d,\gamma)^{4}He$
Transfer reactions $^{2}H(d,p)^{3}H$, $^{2}H(d,n)^{3}He$

K.Arai, S.Aoyama, Y.S., P.Descouvemont, D.Baye, PRL107 (2011)

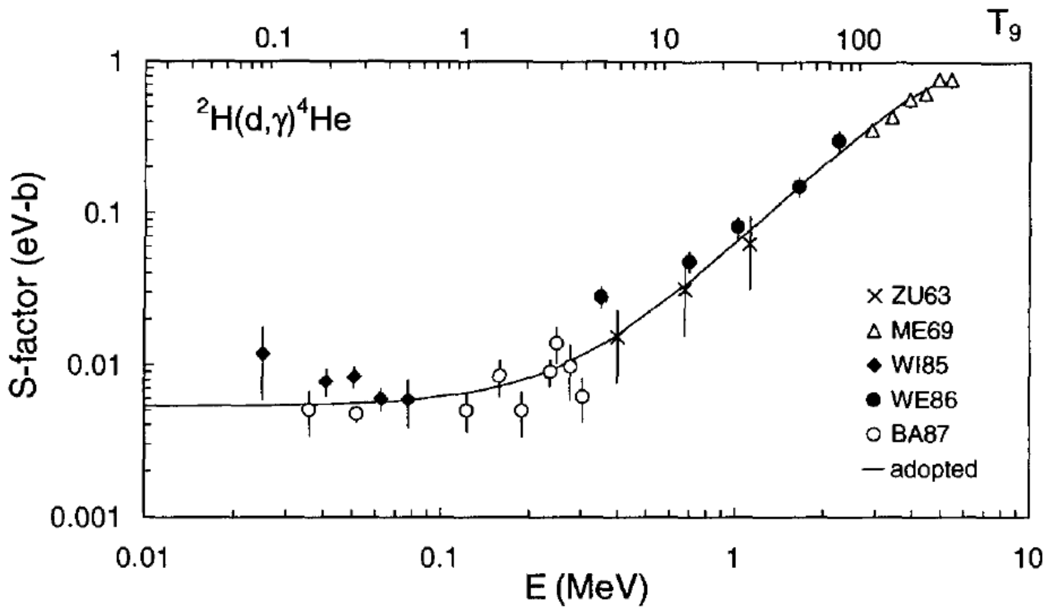

Deuterons in primordial nucleosynthesis of ^{4}He:

$^{2}H(d, p)^{3}H$, $^{2}H(d, n)^{3}He$
$^{3}H(d, n)^{4}He$, $^{3}He(d, p)^{4}He$

Radiative capture at astrophysical energy

$^{2}H(d,\gamma)^{4}He$ at astrophysical energy

E2 transition dominance

Initial channel $^{2I+1}L_J$ I: channel spin =0,1,2 $\ell \leq 2$

Identical bosons

channel \ J^π	0^+	1^+	2^+	0^-	1^-	2^-
$d(1^+)+d(1^+)$	$^1S_0$ $^5D_0$	$^5D_1$	$^5S_2$ $^1D_2$ $^5D_2$	$^3P_0$	$^3P_1$	$^3P_2$
$t(\frac{1}{2}^+)+p(\frac{1}{2}^+)$, $h(\frac{1}{2}^+)+n(\frac{1}{2}^+)$	$^1S_0$	$^3S_1$ $^3D_1$	$^1D_2$ $^3D_2$	$^3P_0$	$^1P_1$ $^3P_1$	$^3P_2$

At extreme low energy S-wave is predominant $\longrightarrow$ $J^\pi=0^+$, 2^+

Other transitions: E1 ($^3P_1$), M1 ($^5D_1$)

No tensor force $\longrightarrow$ No D states in ^2H and ^4He $\longrightarrow$ No S-wave E2 transition but D-wave E2 transition

Sensitive to tensor force

Realistic calculation is hard

H.J.Assenbaum, K.Langanke, PRC36(1987)

A.Arriaga, V.R.Pandharipande, R.Schiavilla, PRC43(1991)

K.Sabourov et al., PRC70(2004)

${}^1S_0$ $d{+}d$ elastic-scattering phase shift

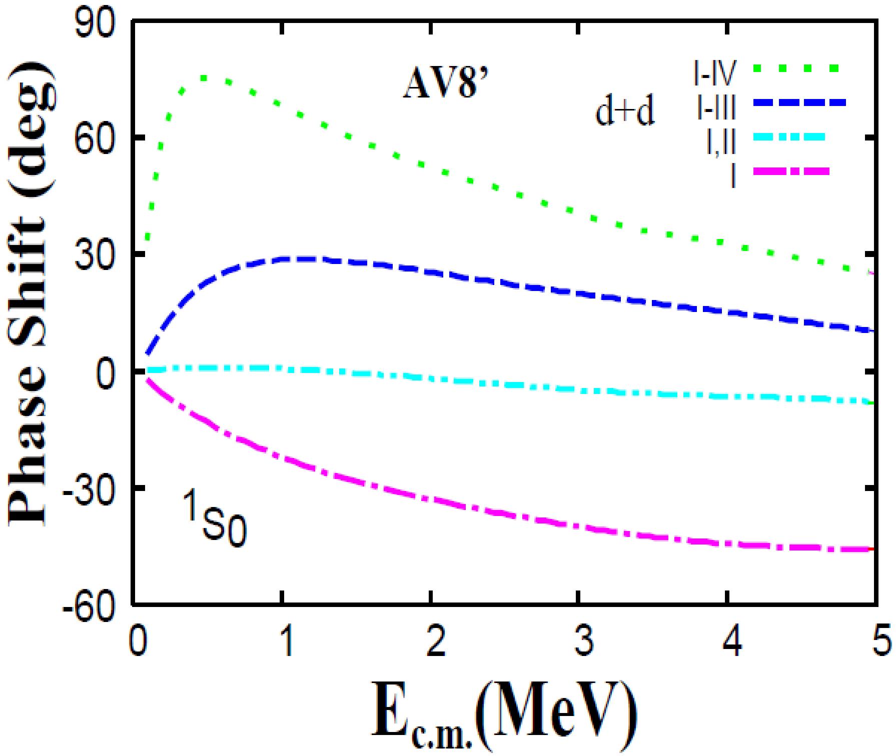

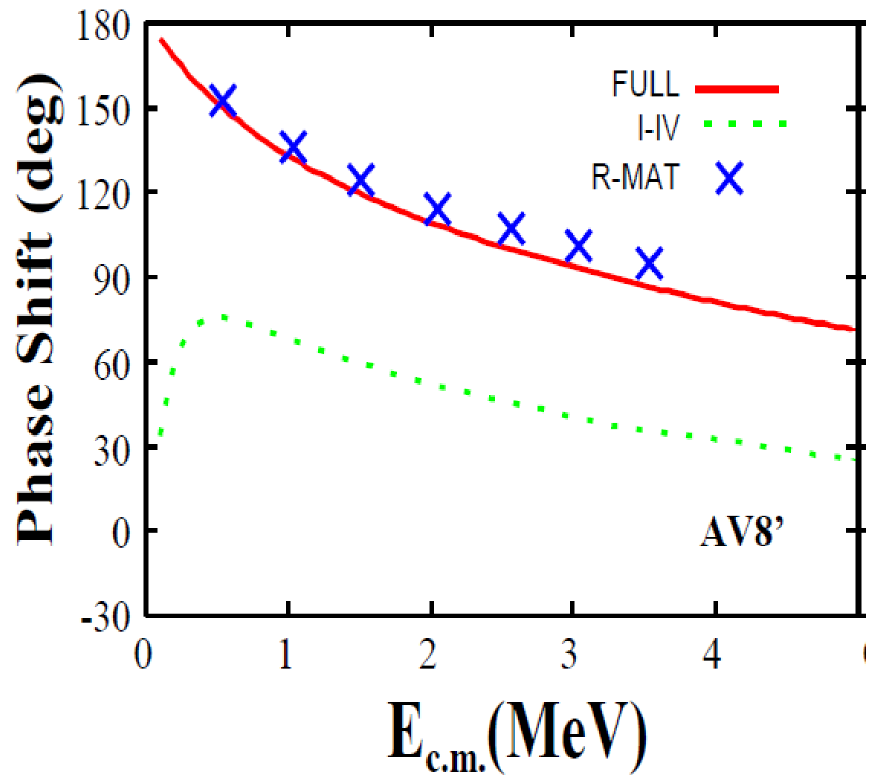

S.Aoyama, K.Arai, Y.S., P.Descouvemont, D.Baye, Few-Body Systems, accepted

MRM results

AV8', G3RS reproduce S-factor, but MN fails at E< 0.3MeV

Three initial dd channels: at E< 0.3 MeV $^5S_2$ dominates giving flat pattern

at E> 0.3 MeV $^1D_2$ dominates

$^5D_2$ minor contributions

$$|^5S_2 : J = 2 > \;\sim\; (1 - P_D(d))|L = 0, S = 2 > \;+\; \sqrt{2P_D(d)}\left\{\sqrt{\frac{1}{5}}|L = 2, S = 0 > + \ldots\right\}$$

$$|^4\mathrm{He} : J = 0 > \;\sim\; \sqrt{1 - P_D(\alpha)}|L = 0, S = 0 > \;+\; \sqrt{P_D(\alpha)}|L = 2, S = 2 >$$

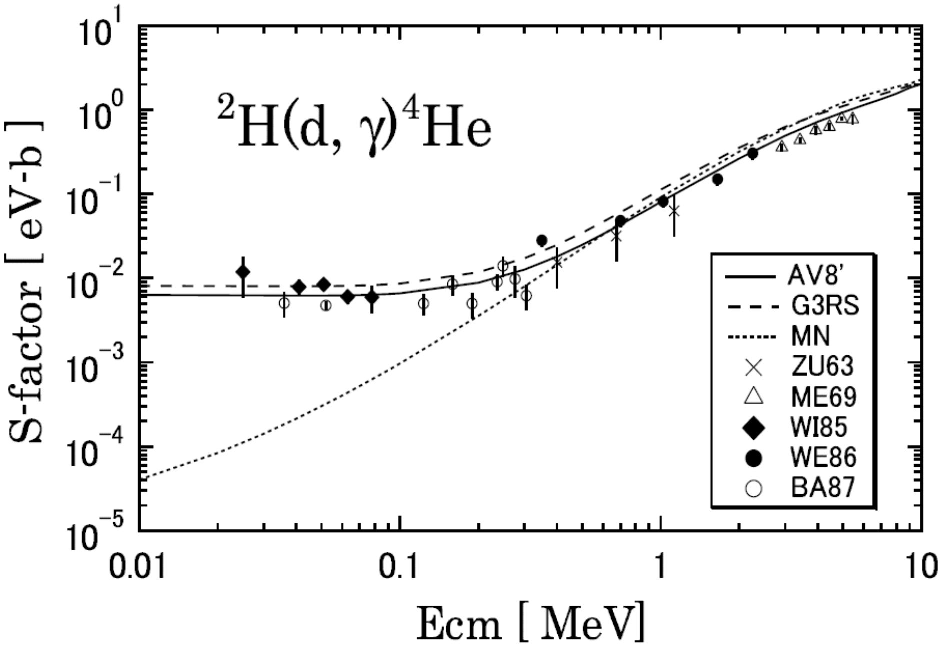

Contribution of three dd channels

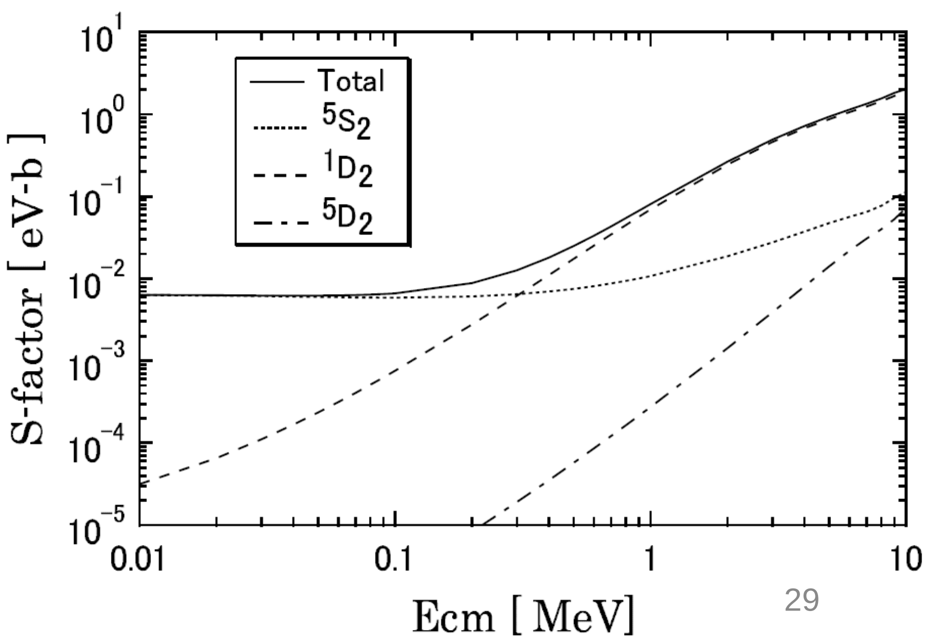

Transfer reactions

$J^\pi = 0^\pm,\ 1^\pm,\ 2^\pm$ states are included

Realistic potentials reproduce S-factors very well
MN potential gives too small values

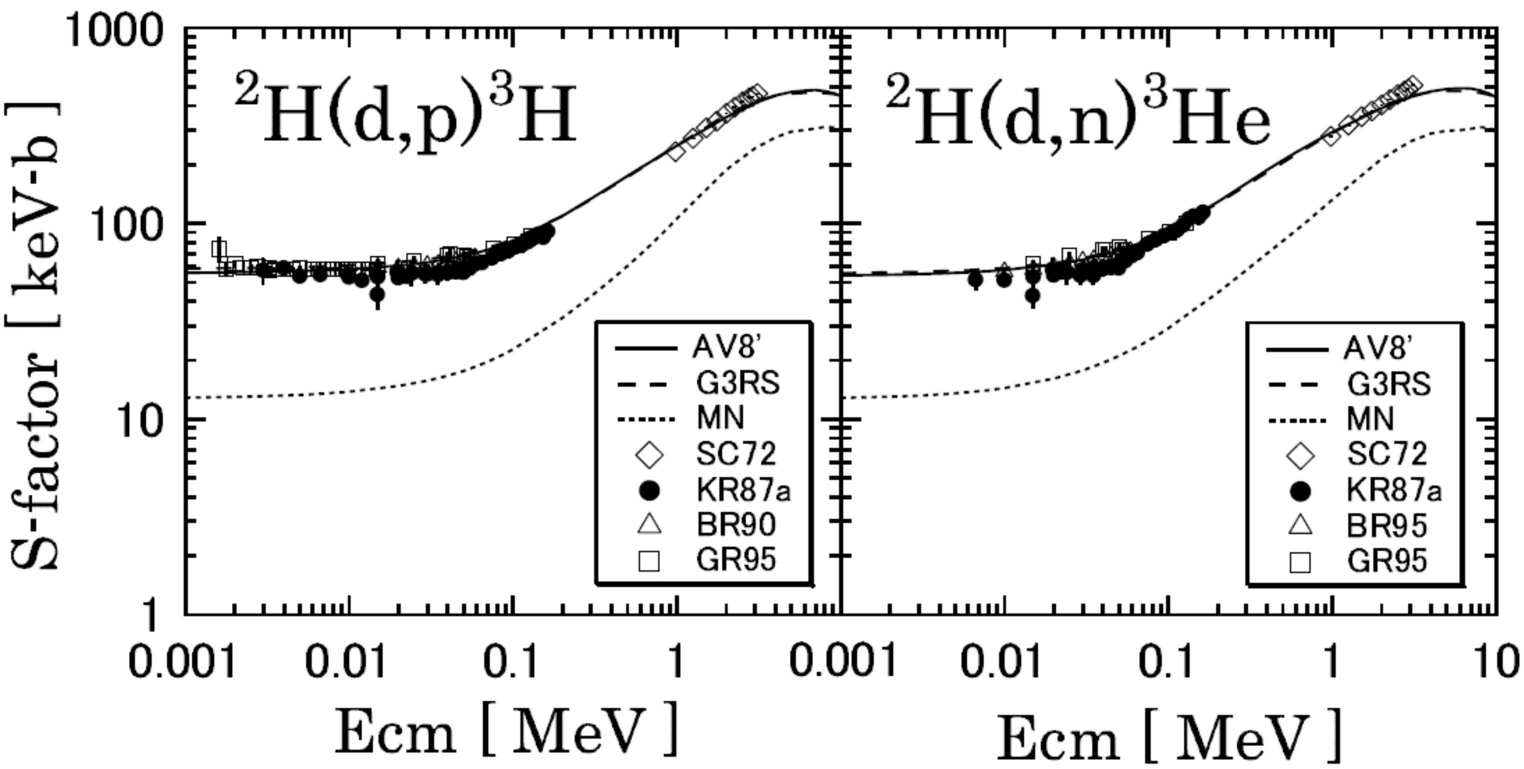

Decomposition of cross sections

2^+ contribution is largest below 60 keV
Among 6 paths for 2^+, ${}^5S_2 \longrightarrow {}^3D_2$ dominates at low energies

$$|tp : {}^3D_2 > \sim \sqrt{1-P_D(t)}|L=2, S=1> + \sqrt{P_D(t)}|\ldots>$$

Main path is from |L=0,S=2> to |L=2,S=1>
Tensor force is responsible

$^2\mathrm{H}(d,p)^3\mathrm{H}$

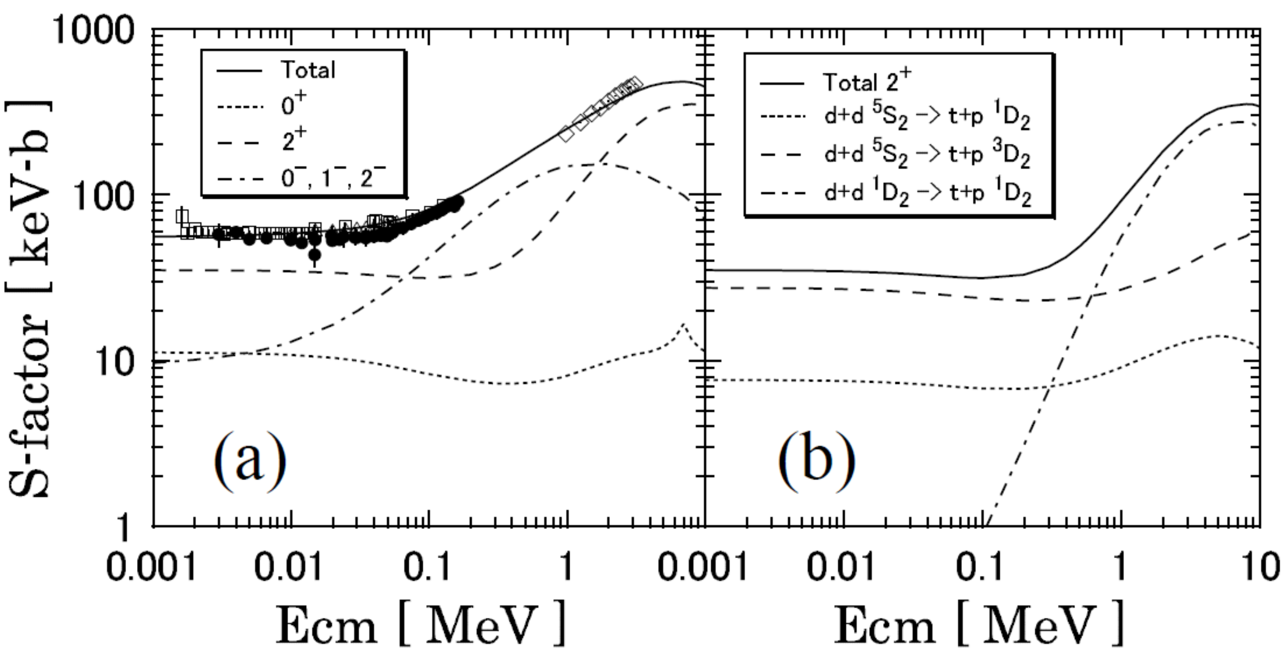

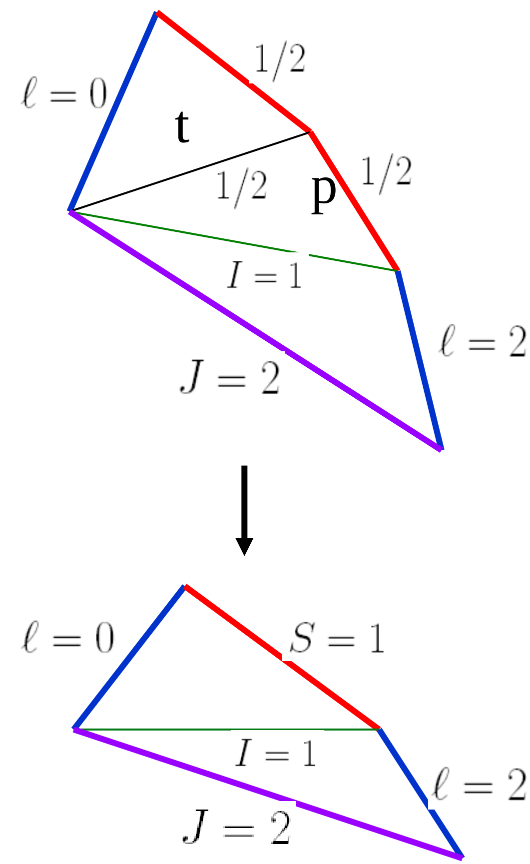

Difficulties in three-body continuum

Hyperspherical harmonics method

Hyperspherical coordinate

Extension of $\boldsymbol{r} = (r, \theta, \phi)$

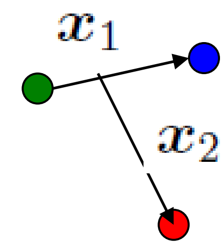

$$\rho = \sqrt{x_1^2 + x_2^2} \qquad \Omega_x \, (\alpha, \theta_1, \phi_1, \theta_2, \phi_2\,)$$

$$\alpha = \arctan(x_2/x_1)$$

$$T_1 + T_2 + T_3 - T_{\rm cm} = -\frac{\hbar^2}{2m}\left(\frac{\partial^2}{\partial\rho^2} + \frac{5}{\rho}\frac{\partial}{\partial\rho} - \frac{1}{\rho^2}\mathcal{K}^2\right)$$

$$\mathcal{K}^2\,\mathcal{F}^{\ell_1\ell_2}_{KLM}(\Omega_x) = K(K+4)\,\mathcal{F}^{\ell_1\ell_2}_{KLM}(\Omega_x) \qquad K = \ell_1 + \ell_2 + 2n$$

Symmetry adaptation $\quad \Phi_{iKLM} = \sum_{\ell_1\ell_2} C^{(i)}_{\ell_1\ell_2}\mathcal{F}^{\ell_1\ell_2}_{KLM}(\Omega_x)$

$$H\Psi_{LM} = E\Psi_{LM} \qquad \Psi_{LM} = \rho^{-\frac{5}{2}}\sum_{iK} f_{iK}(\rho)\Phi_{iKLM}$$

Coupled equation

$$-\frac{\hbar^2}{2m}\Big(\frac{d^2}{d\rho^2}-\frac{(K+\frac{3}{2})(K+\frac{5}{2})}{\rho^2}+k^2\Big)f_{iK}(\rho)+\sum_{i'K'}\langle\Phi_{iKLM}|V|\Phi_{i'K'LM}\rangle f_{i'K'}(\rho)=0$$

Coupling in potential energies

Nuclear part $\sim\mathcal{O}(\frac{1}{\rho^3})$ at large ρ

Coulomb part $\dfrac{Q^L_{iK,i'K'}}{\rho}$

For K=20, Q=35 MeV, ρ>> 300 fm
in order for the Coulomb pot. to dominate
Still Coulomb coupling is present

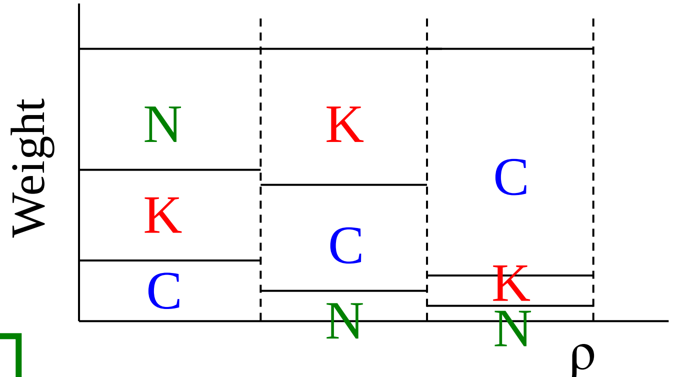

What is the asymptotic form of $f_{iK}(\rho)$?
How to solve the coupled equation?

Conclusion

Exploitation of bound state methods in continuum problems

photoabsorption of ^{4}He

CSM with full final states configurations

Consistency with the inverse reaction dynamics

d-induced reactions on ^{2}H

Microscoic R-matrix method with the inclusion of distorted configurations

Tensor force in ^{2}H(d,γ)^{4}He and ^{2}H(d, p)^{3}H, ^{2}H(d, n)^{3}He

Further study for three-particle continuum problems